



Nanomaterials and Crystals of Topological Insulators and Topological Crystalline Insulators

M. Saghir¹, M.R. Lees, S.J. York, S.A. Hindmarsh, A.M. Sanchez,
M. Walker, C.F. McConville and G. Balakrishnan²

Abstract | Topological insulators (TIs) and topological crystal insulators (TCIs) are a new class of materials that exhibit exotic surface properties. It is thought that these properties are easier to detect if the materials have a high surface-area-to-volume-ratio. We present optimised growth methods to obtain high quality nanomaterials of a number of TCI materials, which have been grown from powdered bulk crystals using a vapour-liquid-solid (VLS) technique. Nanomaterials of SnTe, $Pb_{1-x}Sn_xTe$ and $Pb_{1-x}Sn_xSe$ have been produced and detailed characterisation of the bulk crystals and the nanomaterials through x-ray diffraction, microscopy techniques and EDX analysis are presented. Finally, UHV surface preparation techniques for SnTe microcrystals are presented. Such methods can be used to facilitate direct in-situ measurements of the band structure of TIs and TCIs using techniques such as angle-resolved photoemission spectroscopy (ARPES).

1 Introduction

The exotic surface state that topological insulators and topological crystalline insulators possess has been a driving force in the research into these materials. These new states of matter have surface states that can be difficult to detect, and one proposed method to address this is to reduce the surface area to volume ratio of the materials being investigated for the topologically protected states. Investigating nanomaterials allows easier detection of such signals. Furthermore, it opens up a range of transport measurements that can be conducted to measure the properties of the materials and to potentially exploit those in new and novel devices. A number of growth processes that describe the methods required to obtain a variety of morphologies on the nanoscale have been published. The second generation bismuth based TIs were converted into nanomaterials using simple exfoliation techniques with Scotch tape, a method widely used to isolate layers of graphene. An alternative approach is to grow the nanomaterials from a powder of the material. This is usually done using a vapour-transport growth technique coupled with a gold catalyst to promote growth. For instance, nanowires and nanoribbons

of Bi_2Te_3 can be grown using a simple tube furnace setup through a vapour-liquid-solid mechanism.

Topological crystalline insulators (TCIs) are a new subset of materials first predicted through theory,¹⁻⁵ and later observed in experiments in bulk crystals of the IV-VI semi-metal SnTe showing band degeneracy.⁶ SnTe is a narrow-gap IV-VI semiconductor with a rock salt cubic structure (lattice constant, $a = 0.63$ nm), and was the first material confirmed to be a TCI by angle-resolved photoemission spectroscopy (ARPES). The band degeneracy observed in TCIs are protected by rotational and mirror symmetry, in place of the role played by time-reversal symmetry in TIs.⁷⁻¹⁰ ARPES is one measurement technique that can be used to reveal the exotic surface states of these materials. Measurements to date have been performed only on the surfaces of cleaved bulk crystals or thin films.¹¹ ARPES performed on SnTe has been reported to show Dirac cone surface states.¹²

The effect of substituting Sn in PbTe and PbSe has been explored and it was suggested that by introducing strain into the lattice of these materials, a band inversion could be induced, thereby changing the trivial insulating nature of the materials to topologically non-trivial.¹⁰

ARPES: allows for the direct experimentation of the distribution of electrons in reciprocal space.

The University of Warwick,
Department of Physics,
Coventry, CV4 7 AL,
United Kingdom.

Corresponding Authors:
¹m.saghir@warwick.ac.uk,
²G.Balakrishnan@warwick.ac.uk.

As a result, in the solid solutions $\text{Pb}_{1-x}\text{Sn}_x\text{Te}$ and $\text{Pb}_{1-x}\text{Sn}_x\text{Se}$, TCI surface states have been experimentally observed.⁹⁻¹¹ The TCI nature of these materials is unaffected by mixing disorder of the system.¹² Further experimental evidence obtained using spin-resolved photoelectron spectroscopy (SRPES) has led to the observation of spin textures for the (001) metallic surfaces in both $\text{Pb}_{0.73}\text{Sn}_{0.27}\text{Se}$ and $\text{Pb}_{0.60}\text{Sn}_{0.40}\text{Te}$.^{13,14}

Unlike in the case of SnTe , where the experimental observation of the TCI states can be difficult due to p-type nature of the material, the tunable nature of the chemical potential to n and p-type in $\text{Pb}_{1-x}\text{Sn}_x\text{Te/Se}$ makes these compounds more suitable for experimentally observing the TCI states, thus providing the motivation for the study of these materials.¹⁴

The resulting solid solution upon substitution, $\text{Pb}_{1-x}\text{Sn}_x\text{Te}$, is a narrow band semiconductor with a tunable electronic structure based on the Sn/Pb ratio;⁸ the structure being cubic for all Sn substitutions. For Sn substitution of upto $x \leq 0.4$ in $\text{Pb}_{1-x}\text{Sn}_x\text{Se}$, the structure remains cubic, similar to that of PbSe , whilst the other end member SnSe adopts an orthorhombic structure.

For both $\text{Pb}_{1-x}\text{Sn}_x\text{Te}$ and $\text{Pb}_{1-x}\text{Sn}_x\text{Se}$, the location of the band inversions is analogous to the material SnTe . The introduction of Sn atoms allows for the closing of the band gap, producing a Dirac state. For $\text{Pb}_{1-x}\text{Sn}_x\text{Te}$, the onset for the critical transition from a trivial to non-trivial insulator occurs at a Sn substitution of $\sim x = 0.25$ and the optimum point of this transition is $x = 0.4$.¹⁵⁻¹⁷ A TCI phase onset is observed in $\text{Pb}_{1-x}\text{Sn}_x\text{Se}$ for x values between 0.18×0.3 . This transition is further dependent on

a critical temperature, upto $T_c = 250$ K,¹⁶ and the TCI transition is not observed above this critical temperature.

2 Synthesis

2.1 Crystals

Crystal boules of SnTe were produced using a modified Bridgman following the procedure described by Tanaka et al. Several samples of SnTe were synthesised starting from high purity elements (99.99 % pure) that were mixed in varying ratios ($\text{Sn}:\text{Te} = 51:49, 50:50$ and $49:50$). The Pb-Sn-Te and the Pb-Sn-Se crystal boules were also synthesized using the same procedure,¹ starting with high purity Pb and Sn shot (Alpha Aesar 99.99 %) and powders of Sn and Se (Alpha Aesar 99.99 %). For $\text{Pb}_{1-x}\text{Sn}_x\text{Te}$, an optimum Sn substitution level of $x = 0.4$ was synthesized and for $\text{Pb}_{1-x}\text{Sn}_x\text{Se}$, three different Sn substitution levels $x = 0.18, 0.23$ and 0.30 were made. Following the crystal growth, to check the phase purity, a small section of the boules was finely ground and powder x-ray diffraction patterns were obtained using a Panalytical X'Pert Pro system with monochromatic $\text{CuK}\alpha 1$ radiation. X-ray Laue diffraction was performed on the crystal boules and across the faces of cleaved sections of the boule to check the quality of the crystals produced. Finally, the stoichiometry was determined using an **EDAX EBSD** system installed alongside a Zeiss SUPRA 55-VP scanning electron microscope.

2.2 Nanomaterials

Figure 1 shows a schematic of the furnace used to grow nanomaterials. The **VLS** method was used

EDAX EBSD: Energy dispersive x-ray analysis (EDAX, EDX) can be used to determine the composition of materials. Electron backscatter diffraction (EBSD) can be used to ascertain the crystallographic orientation.

VLS: The vapour-liquid-solid method is a growth process where a gaseous vapour forms a liquid alloy with a catalyst which promotes the growth of nanomaterials.

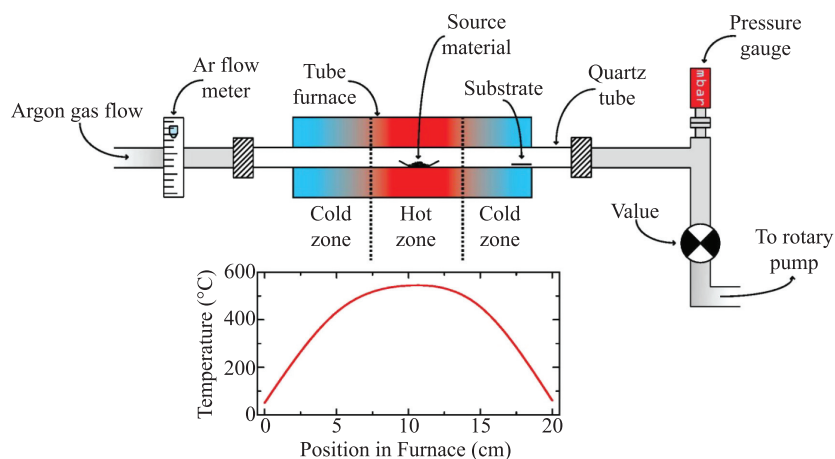


Figure 1: A schematic of a typical growth furnace used to grow nanomaterials. A growth profile can be seen showing sharp temperature gradient. Bulk crystals are powdered and used as source material, which is placed in the centre of the furnace. A substrate is placed downstream and is the site at which nanogrowth occurs. An argon gas flow is established to provide an inert atmosphere during growth and to act as a carrier gas for the source material.

for the growth of nanomaterials for all the materials studied which has been used by many in the past to grow nanomaterials.^{18–22} This process involves the heating of finely ground powder, which is placed in the central hot zone of the growth furnace. Under an argon flow, which acts as a carrier gas and to provide an inert atmosphere during growth, the source material flows downstream to a cooler region in the growth furnace. A substrate placed downstream allows for the nucleation of the source material to form nanomaterials on the substrate surface.

For SnTe nanomaterials silicon substrates were prepared using two methods depending on the SnTe morphologies desired. Au nanoparticles were used as a precursor for nanowire growth, while to promote the growth of microcrystals a smooth Au layer deposited onto the substrate was used. For the first method, the silicon substrate was dipped into and immediately removed from a sodium citrate solution containing 20 nm gold nanoparticles (Sigma Aldrich). With the substrate placed horizontally, the solution was allowed to evaporate in air at room temperature for approximately 30 minutes. As the substrates dried, evenly spaced gold nanoparticles were observed across the substrate surface using an SEM. For the second procedure, a thermal evaporator was used to deposit a 50 to 100 nm layer of gold onto the silicon substrate to act as a catalyst for growth.

For the nanomaterial growth of the Pb-Sn-Te and Pb-Sn-Se, the preparation of the silicon substrates used for growth involved a two step process. First, the silicon wafer substrates (approx. 5 mm × 30 mm) were cleaned using a 50:50 mixture of acetone and isopropan-2-ol. These were then allowed to dry naturally in air before suspending a sodium citrate gold nanoparticle buffer solution on the surface of the substrates (Alpha Aesar 20 nm gold nanoparticles). The buffer was held in position by the surface tension of the solution on the substrates, and the solution then allowed to

evaporate in ambient room temperature conditions. We found that the Au nanoparticles dispersed on the surface with a density of $\approx 5/\mu\text{m}^2$.

For all the materials, about 5 to 50 mg of the powdered source material was placed at the centre of an alumina-silicate boat, which in turn was placed in the centre of the ‘hot zone’ of a 20 cm tube furnace. The parameters used for the growth of the different materials are given in Tables 1 and 2, for SnTe, Pb-Sn-Te and Pb-Sn-Se respectively. For SnTe, about 0.05 g of the boule with the nominal starting composition 51:49 was ground into fine powder and placed in an alumina-silicate boat to act as the source material for the growth. The silicon substrates used were 50 mm × 5 mm strips of silicon wafer, cleaved and cleaned using a solvent mixture of 50:50 isopropan-2-ol and acetone. The silicon substrate was blow dried using nitrogen gas.

The growth furnace is normally ramped up to the growth temperature very rapidly and a carrier gas such as Argon is used to suppress oxides growth. For the growth of SnTe nanomaterials, the source powder was kept at a temperature of 540 °C, while the substrate was kept downstream at around 300 °C. The growth was conducted in a flow of argon gas of 35 sccm for a period of 120 min. The growth of $\text{Pb}_{0.80}\text{Sn}_{0.20}\text{Te}$ and $\text{Pb}_{1-x}\text{Sn}_x\text{Se}$ nanomaterials was carried out at ~ 540 °C in 25 minutes under a flow of argon. The furnace remained at this temperature further for 120 minutes at which point it was allowed to cool to room temperature naturally. The temperature of the ‘cold zone’ where substrates were placed for micro and nanomaterial growth was ≈ 300 °C.

Various parameters were refined and optimized to find the best conditions to obtain high quality nanomaterials with good yield. This involved performing over 30–40 experiments for each material, adjusting the temperature of the hot zone as well as substrate position and argon flow rate, and varying the substrate preparation to get

SEM: Scanning electron microscopy (SEM) is a microscopy characterisation technique.

sccm: Standard Cubic Centimeters—a measure of gas flow

Table 1: Representative atomic compositions of the bulk $\text{Pb}_{0.60}\text{Sn}_{0.40}\text{Te}$ and $\text{Pb}_{1-x}\text{Sn}_x\text{Se}$ crystal boules are shown below. The data was obtained using EDX analysis of the bulk crystals. Lattice parameters for the powdered sections of the crystal boules obtained using powder XRD are also presented. The lattice parameters obtained show a slight discrepancy when compared to previously published data.²¹ This discrepancy may be possible due to the strain in the samples. Further studies are required to investigate this.

Nominal starting composition	Atomic Percent (%)				Lattice parameter (Å)
$\text{Pb}_{0.60}\text{Sn}_{0.40}\text{Te}$	29(2)	21(2)	50(2)	100	6.420(0.020)
$\text{Pb}_{0.82}\text{Sn}_{0.18}\text{Se}$	41(2)	9(2)	50(2)	100	6.147(0.004)
$\text{Pb}_{0.77}\text{Sn}_{0.23}\text{Se}$	40(2)	11(2)	48(2)	100	6.147(0.005)
$\text{Pb}_{0.07}\text{Sn}_{0.30}\text{Se}$	34(2)	16(2)	49(2)	100	6.146(0.008)

XRD: X-ray diffraction is a x-ray crystallography characterisation technique.

Table 2: Growth parameters and results for the optimum growth of SnTe and PbSnTe nanowires. Notable results are shown for all three materials (SnTe, Pb-Sn-Te and Pb-Sn-Se)

Source Material	Mass (g)	Catalyst	Ar Flow Rate (sccm)	Hot Zone (source material) Temp (°C)	Cold Zone (substrate) Temp (°C)	Growth Duration (min)	Result	Composition
SnTe	0.05	Au nanoparticles	35	540	300	120	Thin crystalline nanowires	Sn ₅₀₍₂₎ Te ₅₀₍₂₎
SnTe	0.05	Sputtered Gold	35	540	300	>120	Multiple nucleation sites that have merged to form a thick layered growth.	Sn ₅₀₍₂₎ Te ₅₀₍₂₎
SnTe	0.05	Au nanoparticles	35	560	320	120	Thicker nanowires and microcrystals	Sn ₅₀₍₂₎ Te ₅₀₍₂₎
Pb _{0.60} Sn _{0.40} Te	0.05	Au nanoparticles	35	540	300	125	Thin cuboidal nanowires with distinct cubic faces.	Pb _{0.77(2)} Sn _{0.23(2)} Te
Pb _{0.60} Sn _{0.40} Te	0.05	Au nanoparticles	35	540	320	125	Thick microcrystals	Pb _{0.60(2)} Sn _{0.40(2)} Te
Pb _{0.07} Sn _{0.30} Se	0.05	Au nanoparticles	35	550	305	120	SnSe zigzag nanowires, PbSe microcubes	Sb ₅₀₍₂₎ Se ₅₀₍₂₎ Pb ₅₀₍₂₎ Se ₅₀₍₂₎

the desired structures. The conditions used for the growth of the different materials is given in the tables below.

3 Results and Discussion

3.1 SnTe

The crystal boules when removed from the sealed quartz tubes showed shiny metallic surfaces and cleaved easily along the {100} and {111} planes, revealing flat mirror surfaces. A small section of the crystal boule was ground into a fine powder for powder XRD. The data obtained for the 51:49 composition shows that the SnTe was single phase with no impurities as seen in Figure 2. Compositional analysis using EDAX was performed on several small pieces of crystal obtained from different regions of the boule. The data revealed that the crystals had formed stoichiometrically as can be seen in Table 1. Laue diffraction (Figure 3) was performed on several freshly cleaved surfaces, which revealed well defined sharp diffraction spots.

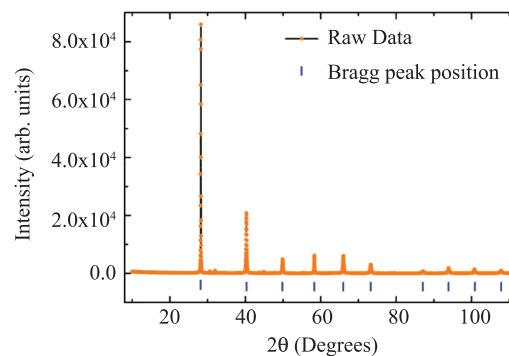


Figure 2: Powder X-ray diffraction pattern of a crushed sample of the as-grown SnTe crystal (composition 51:49). The data obtained (orange) and the expected Bragg peak positions (blue) are shown.

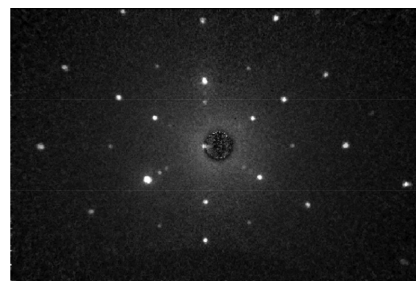


Figure 3: Typical Laue pattern of the as-grown crystal boule. The incident X-ray beam is aligned with the [111] crystallographic direction. The Laue patterns were consistent across the surface of the boule.



Figure 4: (a) Low resolution SEM image of nanowires and microcrystals. (b) Nanowire of SnTe surrounded by Au nanoparticles. (c) High resolution SEM image of the tip of a SnTe nanowire; an alloy can be seen.

After the VLS growth of the nanomaterials, the substrates when inspected by SEM showed long smooth single crystal nanowires. Representative images of the substrate surface are shown in Figure 4 along with a high resolution image of an isolated nanowire. Nanowires were observed to grow in random orientations protruding outwards from the sample surface; typically, the nanowires grown are 200 nm wide and 20 to 50 μm long. EDAX analysis of the nanowire shows that within experimental error the composition is similar to the source material used. From high resolution SEM image of a single isolated nanowire in Figure 4(c), the Au-nanoparticle can be seen at the tip of the nanowire suggesting that it promotes growth, and that growth is nucleated by the Au nanoparticle. The importance of using Au-nanoparticles to catalyze the growth of nanowires is further seen in growths performed without Au-nanoparticles, where no nanowires were observed.

Figure 4(a) shows SnTe nanowires amongst microcrystals that have grown on a silicon substrate. A circular alloy feature can be seen at the tip of the nanowire in Figure 4(c). The nanowires that are grown are typically 20 to 50 μm long and approx. 200 nm wide.

Nanowire formation was best observed in the center of the substrate with microcrystals forming at the warmer end of the substrate (i.e. closer to furnace centre/hot zone). We find that our optimum growth temperature is $540 \pm 20^\circ\text{C}$ and duration is ≈ 120 mins. Using a sputtered layer of gold instead of Au nanoparticles yielded different results. This experimental procedure resulted in the growth of microcrystals in the form of rods and stacks, exhibiting perfectly formed cubic crystal structures of SnTe. A typical SEM image obtained is shown in Figure 5. These were determined to be stoichiometric in composition to the source material. Microcrystal rods were found to form in clusters on the edges of the substrate, protruding out of the surface. Using EBSD, it was found that all the structures grew predominantly in the vicinal $\{001\}$ growth orientation, as seen in Figure 5.

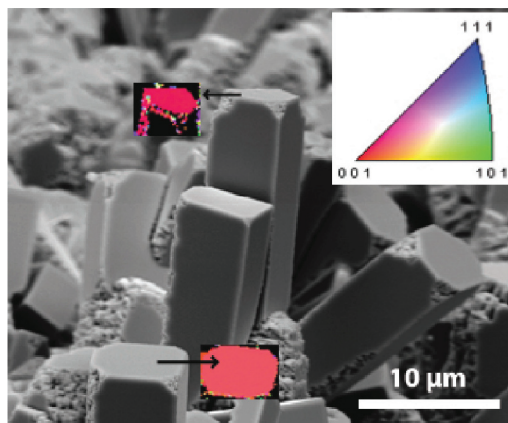


Figure 5: SEM image of SnTe microcrystals. The two red insets placed next to the corresponding microstructures show the EBSD pattern of the growth orientation in the direction normal to the growth axis. This is typically found to be a vicinal $\{001\}$ orientation for the majority of crystals but some show a $\{111\}$ growth plane.

3.2 Pb-Sn-Te/Se

The crystal boules obtained had shiny metallic surfaces when examined visually.

The x-ray powder patterns obtained suggests that the crystals grown are indeed single phase with lattice parameters in good agreement with the expected values. The x-ray Laue diffraction patterns observed revealed sharp spots demonstrating the high crystalline nature of the samples grown, and provided the orientation of the crystals cleaved from the as-grown boules. The EDX results showed that all the crystals grown were of a stoichiometry similar to the nominal starting compositions, within error, as shown in Table 1.

After performing the nanomaterial growth, the substrates were removed from the furnace and upon visual inspection, metallic grey features on the surface of the substrates could be seen. Table 2 shows a summary of the results of the growths performed for the materials. For the growths performed with $\text{Pb}_{1-x}\text{Sn}_x\text{Te}$ nanomaterials in the form of wires were obtained. The growth

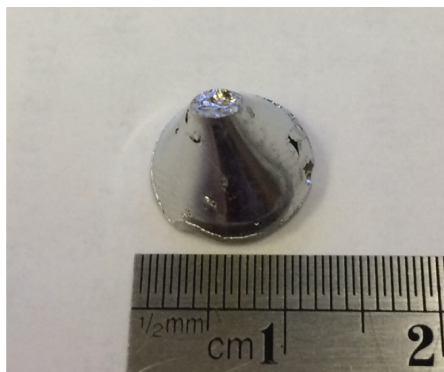


Figure 6: Photographs of an as-grown $\text{Pb}_{0.60}\text{Sn}_{0.40}\text{Te}$ boule with shiny metallic surfaces.

of microcrystals surrounding the free standing nanowires was also observed. For growths with $\text{Pb}_{1-x}\text{Sn}_x\text{Se}$, however, predominantly, microcrystals in the form of cubes were observed with a few nanowires present.

Table 2 below shows the optimum conditions required for the growth of various morphologies of SnTe , PbSnTe and PbSnSe materials. More details can be found in Saghir *et al.*^{23,24}

The nanowires were found to be between 10 and 50 μm long with a typical thickness of ≈ 100 nm. The growth density of the nanowires, observed from SEM, was found to be $\approx 0.40/\mu\text{m}^2$. The TEM image (Figure 7(a)) shows a nanowire with a gold alloy which has formed at the tip, commonly seen in shorter (<4 μm) thinner nanowires (<80 nm). Various stages of the growth from nucleation show that the alloy travels upwards in the direction of growth of the nanowires, which is the typical tip-growth mechanism in these nanowires. Using TEM and SAED, the growth orientation of the crystalline nanowires was determined. SAED studies performed to obtain structural information about the growth orientation of the nanowires showed that the nanowires were highly crystalline in nature and grow along the [100] direction, while TEM results show that some thicker nanowires (>80 nm) grew with a core-shell structure similar to GaAs and ZnO nanowires (Figure 7d).^{22,23} For very long (>4 μm) and thick nanowires (>80 nm), as seen in Figure 7f, no gold alloy was found at the tip of the nanowire, suggesting that the gold nanoparticles eventually become consumed within the body of the longer nanowire. In shorter nanowires (<4 μm), we observed a distinct gold alloy formation at the tip of the nanowire (4a), further demonstrating a change in the growth mechanism of the nanowires from an initial VLS process, which generate shorter and thinner nanowires to a VS process, resulting in longer, thicker wires. EDX obtained in TEM mode

TEM: Transmission electron microscopy (TEM or HR-TEM) is a high resolution microscopy characterisation technique.

SAED: Selected area electron diffraction (SAED) is an electron diffraction characterisation technique.

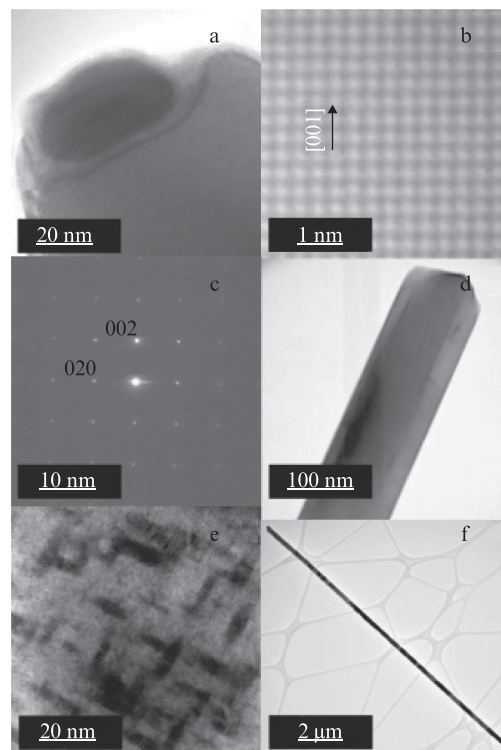


Figure 7: (a) HR-TEM of the gold alloy formed at the tip of a $\text{Pb}_{0.77(2)}\text{Sn}_{0.23(2)}\text{Te}$ nanowire, which has been isolated on a TEM grid with carbon lace. (b) HR-TEM of a $\text{Pb}_{0.77(2)}\text{Sn}_{0.23(2)}\text{Te}$ nanowire. A regular lattice can be seen showing the high crystalline nature of the structure where the lattice parameter equates to 6.497(3) Å. (c) SAED of nanowire. (d) Core-shell growth of nanowire. (e) Guinier-Preston like zones can be seen forming in-plane within the 3D lattice. No defects can be seen in these regions, and compositional analyses reveal that they have the same composition as surrounding areas. (f) A typical long nanowire (> 4 μm).

reveals that the $\text{Pb}_{1-x}\text{Sn}_x\text{Te}$ nanowires have a chemical composition, that is in the region of the critical transition point $x = 0.25$, at which the material changes from a trivial insulator to a TCI. Evidence from various microscopy techniques showed that the materials grew using a VLS technique much like that in the case of SnTe nanowires. The TEM images also showed that the nanowires were structurally similar to their bulk counterparts. Finally, the composition of the nanowires was that at which the material transitioned from a trivial to a non-trivial insulator.

Growth conditions similar to that used for $\text{Pb}_{0.77(2)}\text{Sn}_{0.23(2)}\text{Te}$ nanowires were tried for several compositions of the $\text{Pb}_{1-x}\text{Sn}_x\text{Se}$. For a growth temperature of $\sim 540^\circ\text{C}$, for all Sn compositions attempted, no nanowires or microcrystals were

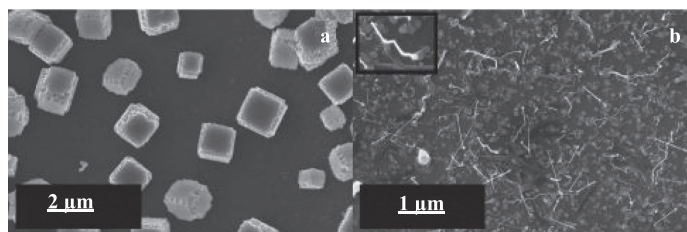


Figure 8: (a) Representative SEM image of the growth of PbSe microcubes. (b) SnSe zig-zag nanowires with the inset for clarity. The thickness of the nanowires obtained for $\text{Pb}_{0.70}\text{Sn}_{0.30}\text{Se}$ are ≈ 40 nm.

obtained. Instead, a thin layer of PbSe material was deposited with trace amounts of Sn. Raising the growth temperatures resulted in the decomposition of $\text{Pb}_{0.70}\text{Sn}_{0.30}\text{Se}$ powder into PbSe microcrystals in the form of cubes and SnSe in the form of zig-zag nanowires, while for temperatures higher than 550 °C, the cubes merged to form a thick continuous layer (Figure 8).

Producing nanomaterials of $\text{Pb}_{1-x}\text{Sn}_x\text{Se}$ using a vapour transport was difficult as the compound decomposed into either PbSe or SnSe nanomaterials.

3.3 Surface preparation of nanomaterials

ARPES is a commonly used technique for investigation of the surface states of TIs; nanomaterials using this technique pose some problems. ARPES is a very surface sensitive measurement technique. As such, the most common approach to study TIs and TCI materials is by in-situ cleaving of bulk crystals or by growing layered materials by MBE for example. We developed a cleaning method that could be applied to materials that have been grown ex-situ of ultra-high vacuum systems.²⁵ The motivation behind finding a method to clean TI and TCI nanomaterials was because the ex-situ growth method described in Figure 1 is a very popular technique for the growth of a range of TIs and TCIs in nanoform. The only way to confirm if these nanomaterials possess TI and TCI behaviour is to perform transport measurement or directly measure the band structure and find signals of band inversion. A UHV in-situ cleaning method was first reported by us for SnTe nanomaterials.²⁵ A XPS cleaning study was conducted, that found that atomic hydrogen cleaning with an anneal cycle (200 °C) gave the best results when cleaning the surface of the samples. The XPS data combined with SEM images of the sample surface before and after atomic hydrogen cleaning can be seen in Figure 9 below.

Through the search of new states of matter, topological insulators, and topological crystalline

insulators, various materials that are thought to be topological superconductors and even combinations of the above, have been discovered and more are being predicted. This re-writes what we know about many materials that have already been exploited in exciting applications.

We now know the importance of having reliable growth methods that can be used for further studies with an eventual aim to exploit the topologically protected states in electronic applications. We have demonstrated the benefits of starting with bulk materials that have been well characterised as precursors in the growth of nanomaterials, and the motivation behind finding repeatable growth procedures of those. The nanostructures produced show interesting properties where now a focus can lie on detecting the enhanced surface states that they exhibit.

Although these surface states are protected from impurities and defects, we are limited by scientific tools that we have for detecting them. Many of the surface probes used today such as ARPES and surface conductivity measurements are heavily dependent on using clean surfaces with known crystallographic orientations. Previous methods used for tackling these problems such as in-situ cleaving have not been ideal. We have presented a surface cleaning procedure that can easily be adjusted for other substrates or samples. Additionally, we have demonstrated that such a cleaning method ensures that the surface topography is unaffected.

4 Summary

We report optimal methods for growth of high quality crystals of the TCIs $\text{Pb}_{0.77(2)}\text{Sn}_{0.23(2)}\text{Te}$ and $\text{Pb}_{1-x}\text{Sn}_x\text{Se}$ ($x = 0.18, 0.23$ & 0.30). From these we determined optimum growth conditions for the formation of nanowires and microcrystals of SnTe, and $\text{Pb}_{0.77(2)}\text{Sn}_{0.23(2)}\text{Te}$. For the solid solution $\text{Pb}_{0.70}\text{Sn}_{0.30}\text{Se}$, we found the compound decomposed to form PbSe microcubes and SnSe zigzag nanowires. Various structures described above were produced using the VLS growth method. We

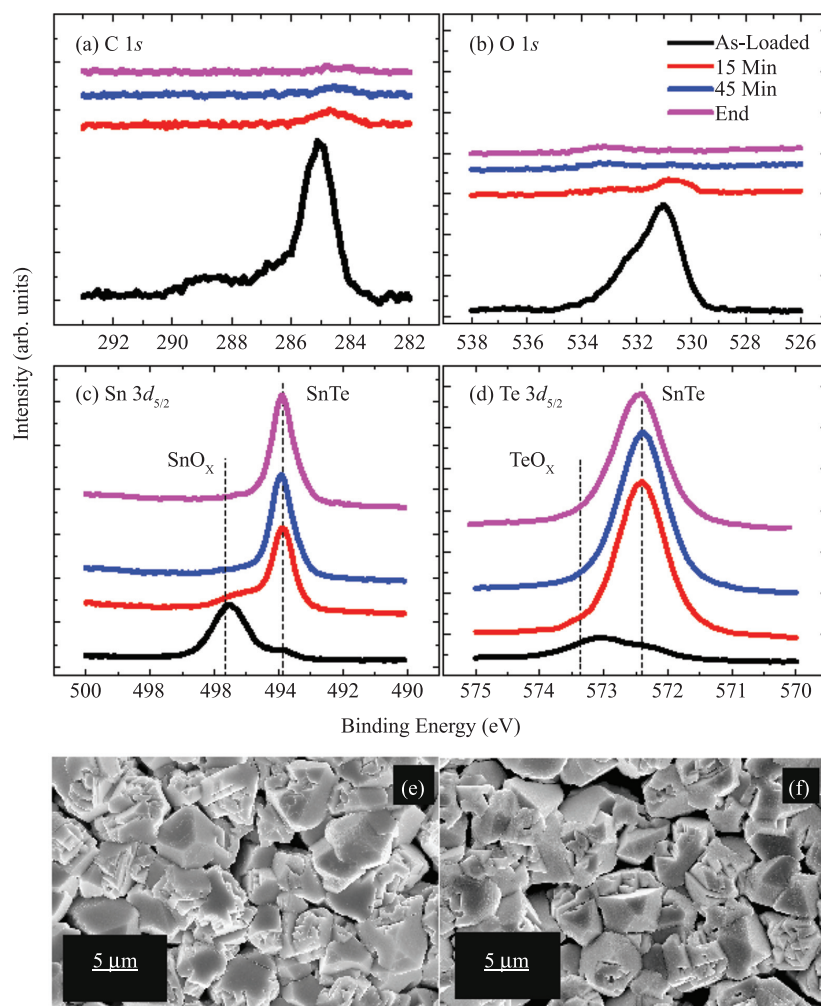


Figure 9: XPS spectra for the (a) C1 s, (b) O1 s, (c) Sn3d_{5/2} and (d) Te3d_{5/2} core-level peaks. Samples were subjected to an atomic hydrogen cleaning cycle at 200 °C and the data presented show chemical shifts for an as-loaded sample (black), the effects after 1 hour (red), 2 hours (blue) and the end of the treatment cycle (purple). (e + f) SEM images of microcrystals pre and post treatment showing no change to the surface morphology.

find that a Au precursor is essential for the growth of both nanowires as well as microcrystals. Growth results are dependent on temperature of the source material, the substrate temperatures correspond to the position of the substrate in the cold zone and the growth duration. We have carried out extensive structural and compositional analyses using x-ray diffraction and EBSD, and investigated the observed structures using both SEM and TEM techniques to analyse and understand the growth mechanisms. Finally, we have produced a reliable cleaning method that can be used to obtain clean surfaces in order to conduct measurements such as ARPES. We believe that the methods and analysis described in this study is easily applicable to many other analogous materials in their morphologies, allowing a pathway to be established to potentially exploit their topological surface states.

Acknowledgements

This work was supported by the EPSRC, UK, Grants EP/L014963/1 and EP/M028771/1. Some of the equipment used in this research was obtained through the Science City Research Alliance (SCRA) Advanced Materials Project 1: Creating and Characterizing Next Generation Advanced Materials Project, with support from Advantage West Midlands (AWM), and was partially funded by the European Regional Development Fund (ERDF). The X-ray photoemission spectroscopy (XPS) data were collected at the University of Warwick Photoemission Facility. The authors thank T.E. Orton and R. Johnston for valuable technical support.

Received 14 March 2016.

References

1. Y. Tanaka, Z. Ren, T. Sato, K. Nakayama, S. Souma, T. Takahashi, K. Segawa and Y. Ando, *Nat. Phys.* **8**, 800–803 (2012).
2. L. Fu, *Phys. Rev. Lett.* **106**, 106802 (2011).
3. D. Hsieh, D. Qian, L. Wray, Y. Xia, Y.S. Hor, R.J. Cava and M.Z. Hasan, *Nature* **452**, 970–974 (2008).
4. D. Hsieh, Y. Xia, L. Wray, D. Qian, A. Pal, J.H. Dil, J. Osterwalder, F. Meier, G. Bihlmayer, C.L. Kane, Y.S. Hor, R.J. Cava and M.Z. Hasan, *Science* **323**, 919–922 (2009).
5. Y. Xia, D. Qian, D. Hsieh, L. Wray, A. Pal, H. Lin, A. Bansil, D. Grauer, Y.S. Hor, R.J. Cava and M.Z. Hasan, *Nat. Phys.* **5**, 398–402 (2009).
6. D. Kong, J.C. Randel, H. Peng, J.J. Cha, S. Meister, K. Lai, Y. Chen, Z.-X. Shen, H.C. Manoharan and Y. Cui, *Nano Lett.* **10**, 329–333 (2010).
7. T.H. Hsieh, H. Lin, J. Liu, W. Duan, A. Bansil and L. Fu, *Nat. Commun.* **3**, 982 (2012).
8. L. Fu and C.L. Kane, *Phys. Rev. B – Condens. Matter Mater. Phys.* **76**, 045302 (2007).
9. S.-Y. Xu, *et al. Nat. Commun.* **3**, 1192 (2012).
10. P.Dziawa, B.J.Kowalski, K.Dybko, R.Buczko, A.Szczerbakow, M. Szot, E. Lusakowska, T. Balasubramanian, B.M. Wojek, M.H. Berntsen, O. Tjernberg and T. Story, *Nat. Mater.* **11**, 2449 (2012).
11. A. Strauss, *Phys. Rev.* **157**, 608–611 (1967).
12. M. Kirkham, X. Wang, Z.L. Wang and R.L. Snyder, *Nanotechnology* **18**, 365304 (2007).
13. S. Ringer and K. Hono, *Mater. Charact.* **44**, 101–131 (2000).
14. Y. Tanaka, T. Sato, K. Nakayama, S. Souma, T. Takahashi, Z. Ren, M. Novak, K. Segawa and Y. Ando, *Phys. Rev. B* **87**, 155105 (2013).
15. B. Wojek, R. Buczko, S. Safaei, P. Dziawa, B. Kowalski, M. Berntsen, T. Balasubramanian, M. Leandersson, A. Szczerbakow, P. Kacman, T. Story and O. Tjernberg, *Phys. Rev. B* **87**, 115106 (2013).
16. D. Kong, J.C. Randel, H. Peng, J.J. Cha, S. Meister, K. Lai, Y. Chen, Z.X. Shen, H.C. Manoharan and Y. Cui, *Nano Lett.* **10**, 329–333 (2010).
17. J.J. Cha, J.R. Williams, D. Kong, S. Meister, H. Peng, A.J. Bestwick, P. Gallagher, D. Goldhaber-Gordon and Y. Cui, *Nano Lett.* **10**, 1076–1081 (2010).
18. J.S. Lee, S. Brittman, D. Yu and H. Park, *J. Am. Chem. Soc.* **130**, 6252–6258 (2008).
19. C.M. Lieber, *MRS Bull.* **28**, 486–491 (2011).
20. P. Yang, *MRS Bull.* **30**, 85–91 (2005).
21. P. Gao and Z.L.J. Wang, *Phys. Chem. B* **106**, 12653–12658 (2002).
22. D.L. Medlin, Q.M. Ramasse, C.D. Spataru and N.Y.C. Yang, *J. Appl. Phys.* **108**, 043517 (2010).
23. M. Saghir, M.R. Lees, S.J. York and G. Balakrishnan, *Cryst. Growth Des.* **14**, 2009–2013 (2014).
24. M. Saghir, A.M. Sanchez, S.A. Hindmarsh, S.J. York and G. Balakrishnan, *Cryst. Growth Des.*, **15**(11), 5202–5206 (2015).
25. M. Saghir, M. Walker, C.F. McConville and G. Balakrishnan, *Appl. Phys. Lett.* **108**, 061602 (2016).



M. Saghir joined the Superconductivity and Magnetism group for his PhD in Oct 2012 under the supervision of Prof. Geetha Balakrishnan and Dr. Neil Wilson. His research focuses on the growth and characterisation of Topological Insulators.



M.R. Lees is a Reader in the Physics Department at the University of Warwick. He previously worked at CRTBT-CNRS, Grenoble, France with Prof. Robert Tournier and also at Blakett Laboratory, Imperial College with Prof. Bryan R. Coles. He has been based at Warwick since 1992.



S.J. York joined Physics Department, Advanced Materials Group in 1983 and since August 2014 he is working as a manager of the Electron Microscopy, RTP. His interest is in Scanning Electron Microscopy.



S.A. Hindmarsh has been at the University of Warwick since September 2010, originally as a Research Technician in the Department of Physics. He now works for the Microscopy Research Technology Platform, with a particular interest in FIB-SEM.



A.M. Sanchez graduated in Chemical Sciences from the University of Granada (Spain) in 1996 and obtained her PhD, "Structural Characterisation of GaN-based heteroepitaxial systems", with highly Honorary distinction from the University of Cadiz in 2001. She spent two years as a research fellow in the Materials Science Department at Liverpool University working on strain measurements in STEM images (obtained in the SuperSTEM at Daresbury labs) and low-loss EELS spectroscopy in semiconductor materials. In September 2009, she was appointed as a Science City Senior Research Fellow in Physics at Warwick University, being part of the Advanced Materials theme.



M. Walker has been a member of the Surface, Interface & Thin Films Group since starting his PhD studies in September 2002. In that time He used the Warwick CAICISS system to study a range of different material systems including metal-metal alloys, metal oxides and semiconductor surfaces. In 2009 he was appointed as a Research Fellow on a new EPSRC grant entitled "Structural and electronic properties of InN surfaces and interfaces".



C.F. McConville is a Director of the Science City Research Alliance (SCRA) project, a collaboration between the University of Warwick and the University of Birmingham, where he also holds an Honorary chair in Physics. He leads the Nanosciences Research Cluster and the Surface, Interfaces & Thin Films Group in the Department of Physics at the University of Warwick. His research interests broadly covers the growth, surface and interface properties of novel semiconducting materials – including oxide, nitride and carbide materials, using a range of experimental techniques to extract physical and electronic structure information of the surfaces and interfaces to compare with the bulk properties of these materials.



G. Balakrishnan is a Professor in the Physics Department at the University of Warwick and has worked at Warwick since 1991. She has worked at the Tata Institute of Fundamental Research in Bombay, India and also as a research fellow at Warwick previous to that. Her research interests are in the growth and investigation of metal and oxide single crystals of superconductors, topological insulators and magnetic materials and also low temperature laboratory measurements and neutron scattering studies. She is a Fellow of the Institute of Physics, UK.